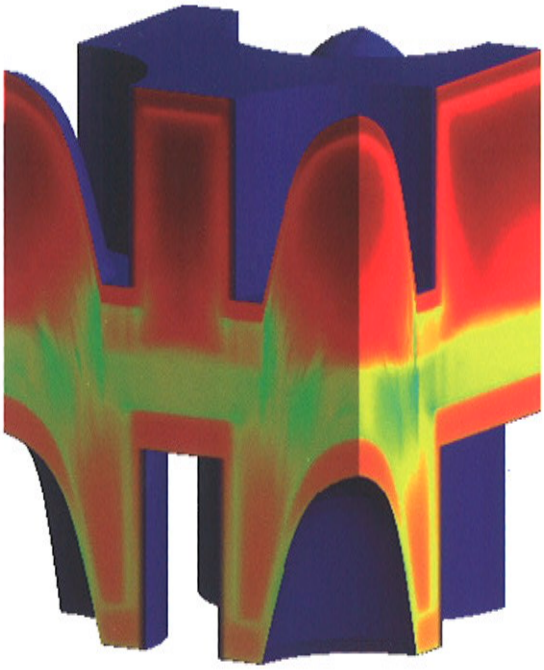

Proceedings of the
14th International Conference on

Numerical Simulation of Optoelectronic Devices

NUSOD 2014

1-4 September 2014

Editors / Chairs:
Joachim Piprek & Julien Javaloyes

Technical Co-Sponsor: The IEEE Photonics Society
IEEE Catalog Number: CFP14817-PRT
ISBN: 978-1-4799-3681-6

$$A^T \hat{x} = \left(\frac{\partial f}{\partial x}\right)^T \quad (6)$$

The system of equation given in (6) is called the adjoint system. Now by substituting (5) into (4), the sensitivity of the objective function is given by:

$$\frac{\partial f}{\partial p_n} = \frac{\partial^e f}{\partial p_n} + \hat{x}^T \left[\frac{\partial b}{\partial p_n} - \frac{\partial A}{\partial p_n} x\right] \quad (7)$$

Since the LU factorization of the matrix A is readily available from solving the original system given in (1), the adjoint variable $\hat{x}$ can be obtained efficiently using (6) by forward–backward substitution. The derivative of the system matrices can be easily obtained using perturbation approach without solving the perturbed system.

$$\frac{\partial A_i}{\partial p_j} \approx \frac{\left(A_i(p_j + \Delta p_j) - A_i(p_j)\right)}{\Delta p_j} \quad (8)$$

Thus, the sensitivity expression in (7) can be solved efficiently.

III. Analytical Approach for Plasmonic Waveguides

Plasmonic waveguides attract the attention in the last decade due to its unique ability to guide the light in subwavelength scale. This unique feature suggests various applications including; optical interconnects and on chip sensing. The plasmonic slot waveguide (PSW) is considered as the most suitable configuration for the aforementioned applications. This waveguide consists of a dielectric slot surrounded by a Nobel metal that exhibits surface plasmon polariton (SPP) resonance at the operating wavelength. PSW also enjoys the unique ability to transmit the light through sharp bends with negligible loss. This feature paves the way for subwavelength functional device size.

Modelling of the plasmonic devices is highly demanding as it requires very fine mesh to model the subwavelength features with good resolution. 3D FDTD modelling of such structures is highly demanding both in time and memory resources. Efficient modelling of the plasmonic devices is essential to allow for fast design optimization.

Due to the unique ability of the PSW to couple light efficiently to orthogonal directions and through sharp bends. Various junctions such as X and T junction can be easily modelled using impedance model to estimate the power coupled to each arm in the junction. This model utilizes the waveguide impedance to estimate the total loading impedance and hence distribute the power accordingly.

The reflections and transmission at each port can be easily estimated using transmission line theory. The reflection and transmitted field can be easily obtained using

$$r_m = \left|\frac{Z_l - Z_m}{Z_l + Z_m}\right| .e^{-2\gamma l_m} \quad \text{, and} \quad (9)$$

$$t = \left|\sqrt{\frac{Z_n}{Z_l}} \times \frac{2\sqrt{Z_m Z_l}}{(Z_m + Z_l)}\right| .e^{-\gamma(l)} \quad (10)$$

where

$$Z_m(\omega, d) = \frac{\beta_{PSW}(\omega, d)\, d}{\omega \varepsilon(\omega)} \quad (11)$$

where Z_m and Z_n are the waveguide impedance of the input port section and the loading sections, l is the length of the waveguide section, and d and the width of the slot.

Using this simple model, the reflection and transmission of each junction can be estimated efficiently [10]. Scattering matrix approach can be utilized to estimate the final response analytically.

The approach has been recently utilized to obtain the analytical expression for various plasmonic devices including; fnano resonator [10], in line filter [11], plasmonic mesh structure [12] and plasmonic power splitter [13].

This approach provides accuracy comparable to the FDTD and alleviates the need for electromagnetic simulation. It also allows for physical insight of the device performance.

IV. Conclusion

Various efficient approaches for modelling photonics and nanophotonic devices are presented and discussed. These approaches open the door for fast and efficient optimization for wide range of applications

References

[1] M. A. Swillam, M. H. Bakr, N. K. Nikolova, and X. Li, "Adjoint sensitivity analysis of dielectric discontinuities using FDTD," *Electromagnetics*, vol. 27, pp. 123 – 140, Feb. 2007.

[2] M. A. Swillam, M. H. Bakr, and X. Li, "Accurate sensitivity analysis of photonic devices exploiting the finite- difference time-domain central adjoint variable method," *Appl. Opt.*, vol. 46 , pp. 1492 – 1499, Mar. 2007

[3] M. A. Swillam, M. H. Bakr, and X. Li, "Full wave sensitivity analysis of guided wave structures using FDTD," *J. Electromag. Waves Applica.* (JEMWA). vol. 22, no. 16, pp 2135-2145, 2008.

[4] M. A. Swillam, M. H. Bakr, and X. Li, "Efficient adjoint sensitivity analysis exploiting the FD-BPM," *IEEE J. Lightwave Technology*, vol. 25, no. 7, pp. 1861 – 1869, July 2007.

[5] M. A. Swillam, M. H. Bakr, and X. Li, "Full vectorial 3D sensitivity analysis and design optimization using BPM," *IEEE J. Lightwave Technology*, vol. 26, no. 5, pp 528 – 536, Mar.. 2008.

[6] M. A. Swillam, M. H. Bakr, and X. Li, "Design optimization of compact wideband optical switch exploiting stair case index MMI," *IEEE J. Lightwave Technology*, vol. 27, no.2, pp 80 – 87, Jan. 15th 2009.

[7] M. A. Swillam, M. H. Bakr, and X. Li, "Efficient design for wideband integrated polarization splitters/combiner," *IEEE J. Lightwave Technology*, vol.28 , no.8, pp. 1176-1183, April 2010.

[8] M. A. Swillam, M. H. Bakr, X. Li and J. Deen, "Efficient sensitivity analysis of time independent Schrödinger equation with application to quantum lasers," *Optics Comm.*, vol. 281, no. 17, pp 4169-4554, 2008.

[9] M. R. AbdelHafez, and M.A. Swillam, "Sensitivity analysis of plasmonic waveguides using FEM," Optics Comm., Feb 2014.

[10] M. A. Swillam, and A. S. Helmy, "Feedback effect in plasmonic waveguides examined using closed form," *Photonics Technology Letters*, vol.19,no. 24, pp 497-499, March 2012.

[11] R. Kotb, Y Ismail, .M A. Swillam, "Integrated Metal-Insulator-Metal Plasmonic Nanoresonator: An Analytical Approach," Progress in electromagnetic research lett , Vol. 43, 83-94, 2013.

[12] C. Lin, M. A. Swillam, and A. S. Helmy, "Analytical model for metal-insulator–metal mesh waveguide architectures," J. Opt. Soc. Am. B, 3157-3169 (2012).

[13] M. Ayad, S. Obayya, M.A. Swillam, "1xN plasmonic power splitters using metal insulator metal configurations," Journal of Lightwave Technology, Accepted.

Simulation of nonlinear optical resonator circuits

T. Van Vaerenbergh, M. Fiers and P. Bienstman
Photonics Research Group
Dept. of Information Technology; Ghent University - imec
Sint-Pietersnieuwstraat 41; B-9000 Ghent, Belgium
Email: thomas.vanvaerenbergh@intec.ugent.be

J. Dambre
Computer Systems Lab
Electronics and Information Systems; Ghent University
Sint-Pietersnieuwstraat 41; B-9000 Ghent, Belgium

***Abstract*—Recently, we proposed a node-based framework to model large circuits of nonlinear photonic components. This flexible tool can be used to simulate circuits that contain a variety of components both in time-domain and in frequency-domain. In this paper, we extend the node-definition of this framework such that that the linear coupling between access waveguides and resonance states in optical resonators can be more efficiently incorporated. We demonstrate that this results in an important decrease of the simulation time in large circuits of nonlinear photonic cavities.**

I. Introduction

Many optical resonators can be described using a Coupled Mode Theory (CMT)-like format for the equations concerning the optical field. For instance, the models that used to describe the dynamics of a passive nonlinear microring [1], [2] or a microdisk laser [3], [4], are CMT-based. In this section we will point out how the framework presented in Ref. [5] can be adapted to CMT-style models, and how this adaptation can in some cases result in an additional increase in simulation speed. For instance, the large circuit simulations done in [2] took advantage of this speed up.

II. Reshaping the System Equation Towards CMT

In [5], the generalized connection matrix $\mathbf{C}_{in,ex}$ models the linear and instantaneous transmission of the waves that originate from a generalized 'external' sources vector $\mathbf{s}_{ext}(t)$ and travel through the components of the circuit. This connection matrix speeds up the time-domain simulations when the inputs of all the memory-containing (MC) components (resonators, lasers, ...) need to be calculated for a given $\mathbf{s}_{ext}(t)$, as it eliminates the memoryless (ML) components (splitters, instantaneous waveguides, ...) from the circuit. One single sparse matrix product

$$\mathbf{s}_{in,MC}(t) = \mathbf{C}_{in,ex}\mathbf{s}_{ext}(t), \quad (1)$$

calculates the inputs of the MC simultaneously for all the nodes. As this improvement in speed is clearly due to the *linearity* of the signal transfer encoded in the scatter-matrix, we will now investigate how additional linear behaviour in the MC node can be exploited to make the framework even more efficient. In CMT models, the light coupling between the optical modes of the cavity and the access waveguides is also linear. Specifically, the CMT equations of a nonlinear resonator i are given by:

$$\frac{d\mathbf{a}_i}{dt} = \mathbf{M}_i\mathbf{a}_i + \mathbf{K}_i^T\mathbf{s}_{i,in} + \mathbf{N}_i(\mathbf{a}, t, ...) \quad (2)$$

The function $\mathbf{N}_i$ describes the nonlinear contribution, e.g., due to changes in absorption or refractive index by the Kerr nonlinearity. If the cavity model contains additional dynamic variables, such as the number of free carriers, or the temperature, these extra equations can as well be shoehorned in the previous matrix format, by extending $\mathbf{K}_i^T$ in the appropriate places with zeros and $\mathbf{M}_i$ with linear contributions of the corresponding Ordinary Differential Equation (ODE), while the remaining nonlinear terms can be incorporated in $\mathbf{N}_i(\mathbf{a}, t, ...)$. More generally, every MC component can be trivially transferred into this format, by extending the original ODE system with additional $\mathbf{M}_i$, $\mathbf{K}_i^T$ and $\mathbf{D}_i$ matrices equal to zero. As we use sparse matrices, these additional zeros have no significant influence on the simulation speed.

Even if the resonator is nonlinear, the coupling of the modes and input signals to the output stays linear:

$$\mathbf{s}_{i,out} = \mathbf{S}_i\mathbf{s}_{i,in} + \mathbf{D}_i\mathbf{a}, \quad (3)$$

We now define the linear coupling matrices $\mathbf{M}$, $\mathbf{K}^T$ and $\mathbf{D}$ for the circuit as a whole. These matrices are block matrices, constructed from the submatrices $\mathbf{M}_i$, $\mathbf{K}_i^T$ and $\mathbf{D}_i$ for all the MC nodes $i \in \{0, ..., N-1\}$. Using the same syntax as before, $\mathbf{M}$ linearly couples the states to the states, $\mathbf{K}^T$ couples the input to the states, while $\mathbf{D}$ couples the states to the output. If we suppose the system has s states, then $\mathbf{M}$ is $s \times s$ dimensional, while $\mathbf{D}$ and K are both $p \times s$ dimensional. Using those matrices, we write down the total ODE of the circuit as:

$$\frac{d\mathbf{a}}{dt} = \mathbf{M}\mathbf{a} + \mathbf{K}^T\mathbf{s}_{in,MC} + \mathbf{N}(\mathbf{a}, t, ...) \quad (4)$$

The generalized source term defined in [5] can be split into two parts: a linear part, related to the linear coupling by D_i of the resonators in the circuit, and an external source term $\mathbf{s}'_{ext}(t)$ of which the linear coupling terms are substracted (e.g., containing the input signals of the sources in the circuit, or the outputs of waveguides with delay or Semiconductor Optical Amplifiers (SOAs)), such that:

$$\mathbf{s}_{in,MC} = \mathbf{C}_{in,ex}\left(\mathbf{D}\mathbf{a} + \mathbf{s}'_{ext}\right). \quad (5)$$

III. Increasing Sparseness

In this subsection, we will use the knowledge of the positions of resonators, detectors and sources in a circuit to make the matrices in the system equations sparser, resulting in a speed improvement of the calculation time.

If a circuit contains cavities with a CMT model, then we know that s'_{ext} will be equal to zero at those port positions. Similarly, port positions of detectors in the circuit will also

978-1-4799-3682-3/14/$31.00

correspond to additional zeros in s'_{ext}. We will now introduce a diagonal $p \times p$ matrix $\mathbf{I}^M_{ex}$, that contains a zero on the diagonal for each port that corresponds to a resonator or a detector. Using this matrix and Eq. (5), assuming that the rows of $\mathbf{D}$ are only nonzero at the port positions of resonators we obtain:

$$\mathbf{s}_{in,MC} = \mathbf{C}_{in,ex}\left[\left(\mathbf{I} - \mathbf{I}^M_{ex}\right)\mathbf{Da} + \mathbf{I}^M_{ex}\mathbf{s}'_{ext}\right]. \qquad (6)$$

The presence of $\mathbf{I}^M_{ex}$ in the previous equation generates additional zeros in the matrix products, making them sparser and hence potentially speeding up the calculations. Hence, $\mathbf{I}^M_{ex}$ can be considered to be some kind of 'mask' matrix.

Additionally, when doing a time-domain simulation, it is not necessary to calculate $\mathbf{s}_{in,MC}$ at the port positions that contain sources (assuming that these sources are not influenced by reflected signals from the circuit, as is the case in most simulations). We will now introduce a second diagonal $p \times p$ mask matrix $\mathbf{I}^M_{in}$, that contains a zero on the diagonal for each port that corresponds to a resonator or a source. By defining $\mathbf{s}'_{in,MC} = \mathbf{I}^M_{in}\mathbf{s}_{in,MC}$ as the vector that monitors the inputs of all the ML nodes, except for the sources and the resonators, we can rewrite $\mathbf{s}_{in,MC}$ to:

$$\mathbf{s}_{in,MC} = \mathbf{s}'_{in,MC} + \left(\mathbf{I} - \mathbf{I}^M_{in}\right)\mathbf{s}_{in,MC}. \qquad (7)$$

Assuming that only the columns of $\mathbf{K}^\mathbf{T}$ corresponding to the resonators are different from zero, $\mathbf{K}^\mathbf{T}\mathbf{s}'_{in,MC} = 0$ and introduction of Eq. (7) in Eq. (4) results in:

$$\frac{d\mathbf{a}}{dt} = \mathbf{Ma} + \mathbf{K}^\mathbf{T}\left(\mathbf{I} - \mathbf{I}^M_{in}\right)\mathbf{s}_{in,MC} + \mathbf{N}(\mathbf{a}, t, ...). \qquad (8)$$

Substitution of Eq. (6) gives:

$$\begin{aligned}\frac{d\mathbf{a}}{dt} =& \left[\mathbf{M} + \mathbf{K}^\mathbf{T}\left(\mathbf{I} - \mathbf{I}^M_{in}\right)\mathbf{C}_{in,ex}\left(\mathbf{I} - \mathbf{I}^M_{ex}\right)\mathbf{D}\right]\mathbf{a} \\ &+ \left[\mathbf{K}^\mathbf{T}\left(\mathbf{I} - \mathbf{I}^M_{in}\right)\mathbf{C}_{in,ex}\mathbf{I}^M_{ex}\right]\mathbf{s}'_{ext} + \mathbf{N}(\mathbf{a}, t, ...), \end{aligned} \qquad (9)$$

while $\mathbf{s}'_{in,MC}$ can be calculated to be:

$$\mathbf{s}'_{in,MC} = \left[\mathbf{I}^M_{in}\mathbf{C}_{in,ex}\left(\mathbf{I} - \mathbf{I}^M_{ex}\right)\mathbf{D}\right]\mathbf{a} + \left[\mathbf{I}^M_{in}\mathbf{C}_{in,ex}\mathbf{I}^M_{ex}\right]\mathbf{s}'_{ext}. \qquad (10)$$

The matrices in Eqs. (9)-(10) can be calculated in advance. Hence, in a time-domain simulation, integration of Eq. (9) can be done by updating only $\mathbf{s}'_{ext}$ instead of $\mathbf{s}_{ext}$. Advantageously, $\mathbf{s}'_{ext}$ will be sparser, and additionally, the output signals at the resonators do not need to be tracked anymore, as their influence on the inputs of other non-resonator MC components is incorporated by the matrix product with $\mathbf{a}$ in Eq. (10). Similarly, in circuits with a lot of resonators and sources, $\mathbf{s}'_{in,MC}$ is a lot sparser than $\mathbf{s}_{in,MC}$.

IV. Applicability of the Extended Framework

Importantly, the previous derivation considers general circuits, that can contain other components than sources, detectors and resonators. Hence, components such as waveguides with delay or SOAs can still be part of the circuit, making this extended framework very flexible.

It depends on the circuit details how much the extended framework improves the simulation speed. In Fig. 1 we illustrate this using two circuits with a significant number of resonators. In Fig. 1(a) we simulate a chain of the inline PhC cavities discussed in [6]. For large chains, using the extended

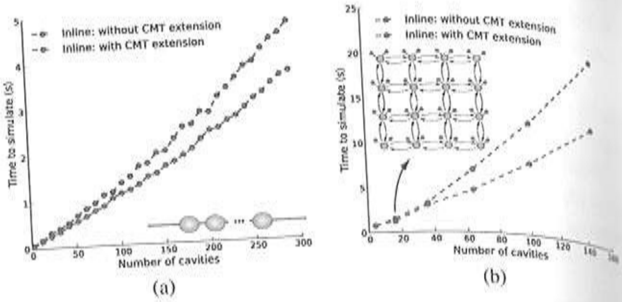

Fig. 1. (left) In a long chain of inline PhC cavities, incorporation of the CMT formalism improves the simulation speed. This simulation is based on the corresponding simulation in [5]. (right) A similar improvement can be seen in a simulation of a nanophotonic reservoir of inline PhC cavities in the topology discussed in [2], [5].

framework results in a 25%-reduction in the number of non-zero elements in the matrix products. As a large part of the simulation time is spent in the calculation of these matrix products, this results in an almost equally large decrease of the total simulation time. In Fig. 1(b) we simulate a large nanophotonic reservoir of PhC cavities. In this case, the relative reduction in calculation time is even stronger. This is mainly due to the large number of sources and detectors in the nanophotonic reservoir, which brings along a lot of unnecessary calculations per time step in the original framework (e.g., propagating nonexistent output signals of the detectors to the sources).

V. Conclusion

By taking benifit of the linear part in the CMT-equations of optical resonators, we showed how the node-based framework proposed in [5] can be optimized for the simulation of large resonator-circuits. Due to the use of sparse matrices, this extension of the framework does not affect the simulation speed of optical components that do not such a linear part. Therefore, the general applicability of the original framework is preserved.

Acknowledgment

This work is supported by the IAP Photonics@be of the Belgian Science Policy Office and the ERC NaResCo Starting grant. T. Van Vaerenbergh is supported by the Flemish Research Foundation (FWO) for a PhD Grant.

References

[1] T. Van Vaerenbergh, et al., "Cascadable Excitability in microrings," Opt. Express 20, 20292–20308 (2012).

[2] M. Fiers, et al., "Nanophotonic reservoir computing with photonic crystal cavities to generate periodic patterns," IEEE Trans. Neural Netw. Learn. Syst. 25, 344–355 (2014).

[3] K. Alexander, et al., "Excitability in optically injected microdisk lasers with phase controlled excitatory and inhibitory response," Opt. Express 21, p.28922-28932 (2013).

[4] T. Van Vaerenbergh, et al., "Excitation transfer between optically injected microdisk lasers," Opt. Express 21, 28922–28932 (2013).

[5] M. Fiers, et al., "Time-domain and frequency-domain modeling of nonlinear optical components on circuit-level using a node-based approach," J. Opt. Soc. Am. B 29, 896–900 (2011).

[6] B. Maes, et al., "Self-pulsing and chaos in series of coupled nonlinear micro-cavities," Physical Review B11 7911 (200911).